ACS APPLIED MATERIALS & INTERFACES

Research Article

www.acsami.org

Magnetoresistance of Drop-Cast Film of Cobalt-Substituted Magnetite Nanocrystals

Shigemi Kohiki,*[,†] Koichiro Nara,[†] Masanori Mitome,[‡] and Daiju Tsuya[§]

[†]Department of Materials Science, Kyushu Institute of Technology, 1-1 Sensui, Tobata, Kitakyushu, Fukuoka 804-8550, Japan

[‡]International Center for Materials Nanoarchitectonics, National Institute for Materials Science, 1-1 Namiki, Tsukuba, Ibaraki 305-0044, Japan

[§]Nanofabrication Platform, National Institute for Materials Science, 1-2-1 Sengen, Tsukuba, Ibaraki 305-0047, Japan

Supporting Information

ABSTRACT: An oleic acid-coated $Fe_{2.7}Co_{0.3}O_4$ nanocrystal (NC) self-assembled film was fabricated via drop casting of colloidal particles onto a three-terminal electrode/MgO substrate. The film exhibited a large coercivity (1620 Oe) and bifurcation of the zero-field-cooled and field-cooled magnetizations at 300 K. At 10 K, the film exhibited both a Coulomb blockade due to single electron charging as well as a magnetoresistance of ∼−80% due to spin-dependent electron tunneling. At 300 K, the film also showed a magnetoresistance of ∼−80% due to hopping of spin-polarized electrons. Enhanced magnetic coupling between adjacent NCs and the large coercivity resulted in a large spin-polarized current flow even at 300 K.

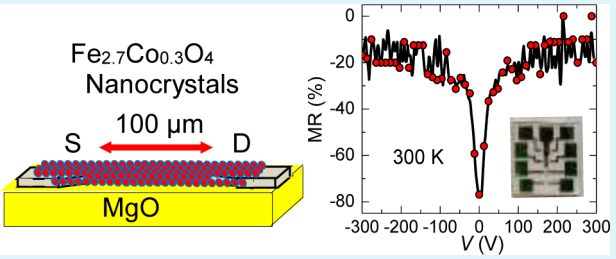

KEYWORDS: *Coulomb blockade, tunnel magnetoresistance, cobalt-substituted magnetite nanocrystal, coercivity, spin-polarized current*

INTRODUCTION

Arrays of ferromagnetic nanocrystals (NCs) isolated within insulating thin layers are known to display both tunnel magnetoresistance (MR) and Coulomb blockade behavior.[1,2] There is great research interest in the MR of NC arrays of the half-metal magnetite (Fe_3O_4) and its analogs for the development of spin-polarized current switching devices which can operate above room temperature (RT).[3,4] In multiple junction systems consisting of arrays of ferromagnetic NCs weakly electrically contacting one another via thin, insulating barriers, electron tunneling between the NCs depends on the alignment of the magnetic moments of adjacent NCs. When the angle between the magnetic moments of adjacent NCs in a three-dimensional (3D) system is denoted by θ, the relative magnetization of the system m is related to θ by $m^2 = \langle\cos\theta\rangle$, and the MR is connected to the spin-polarizability (P) of the charge carriers and m by $\mathrm{MR} \equiv P^2m^2/(1 + P^2m^2)$.[1] MR is also defined experimentally as $\mathrm{MR} = (G_0/G_H) - 1$, where G_0 and G_H are the differential conductance ($G = \mathrm{d}I/\mathrm{d}V$) for nonlinear current and voltage (I−V) characteristics in zero and nonzero magnetic fields (H), respectively. When G is varied from low to high by a nonzero H, which is strong enough to change the configuration of the magnetic moments in the system to be in parallel ($\theta = 0$), the sign of MR becomes negative.

Half-metal Fe_3O_4 is expected to have fully spin-polarized (P = 100%) carriers up to its Curie temperature (≈ 840 K);[5,6] however, the 100% spin-polarizability at high temperatures remains in controversy still now. If the 100% spin-polarizability was preserved even at room temperature (RT), MR for Fe_3O_4 NCs reaches −50% at RT when the condition $m = 1$ is fulfilled. Recently, values of MR = −58% at 200 K and −46% at 295 K were achieved for self-assembled Fe_3O_4 NC arrays.[3] Other than the values reported by Poddar et al. (MR = −300% at 110 K and −125% above 150 K),[7] such magnitudes have no precedent. MR values of −35% at 60 K,[8] −40.9% at 110 K,[9] −11.5% at 100 K,[10] −21% at 130 K, and −13% at 280 K,[11] −17% at 115 K and −7% at RT,[12] and −25% at 250 K[13] have been reported. The rather large MR observed below 130 K reflects an increase in the resistivity due to the Verwey transition in the Fe_3O_4 crystal lattice.[14] An increase in temperature should lessen the m value because thermal energy enlarges the θ value. An enlarged magnetic coercivity (H_c), strong enough to realize the $m = 1$ condition above RT, should provide MR values on the order of −50% for Fe_3O_4 NC arrays. The large MR brings about very high performance for spin-polarized current switching devices.

Cobalt is known as an anisotropic moment carrier. Cobalt-substituted magnetite ($Fe_{3-x}Co_xO_4$) exhibits a large magnetic anisotropy constant (K),[15] and a large H_c has been reported for self-assembled $Fe_{3-x}Co_xO_4$ NC arrays.[16] There are limited reports concerning the magnetic properties of $Fe_{3-x}Co_xO_4$ NCs;[16−18] however, to date, there have been no studies of the magnetoresistance. Since Co^{II} replaces Fe^{II} in Fe_3O_4,[16] self-

Received: February 1, 2014
Accepted: September 26, 2014
Published: September 26, 2014

 © 2014 American Chemical Society

assembled $Fe_{3-x}Co_xO_4$ NC arrays are expected to possess a larger MR than those of Fe_3O_4, even at RT, since a larger H_c enhances the magnetic coupling between adjacent NCs.

As a foundation for a high-performance spin-polarized current switching device, the MR of an oleic acid-coated $Fe_{3-x}Co_xO_4$ NC self-assembled film fabricated via drop casting of colloidal particles was examined at 10 and 300 K. The $Fe_{3-x}Co_xO_4$ NCs were synthesized by refluxing $Fe(acac)_3$ and $Co(acac)_2$ in a solution of dibenzylether mixed with oleic acid. Oleic acid, $CH_3(CH_2)_7CH{=}CH(CH_2)_7COOH$, is an unsaturated carboxylic acid with a *cis*-double-bond "kink" in the middle of its C_{18} tail. The polar headgroup chemisorbs to the hydrophilic surface of the NC, and steric repulsion of the long chain prevents the NCs from agglomerating.[19] Since oleic acid-coated NCs are hydrophobic, the slow drying of a hexane colloidal suspension dropped onto a substrate results in a self-assembled film with hexagonal networks of NCs.[3] This spontaneous self-assembly phenomenon is commonly used to control the arrangement of NCs into hexagonally ordered arrays.[20,21] Geometrically frustrated networks of collinear magnetic moments cause a spin-glass (SG) transition for two-dimensional (2D) ordered NC arrays, and decrease G_0 for spin-polarized current flow. Furthermore, hydrophobization by oleic acid is highly advantageous in preventing the lowering of the observed spin polarization due to surface oxidation.[22] Electron tunneling into a $Fe_{3-x}Co_xO_4$ NC which has been isolated by oleic acid increases the electrostatic charging energy (E_C). Thus, tunneling between adjacent NCs can be blocked at low temperatures and voltages. In this study, at 10 K, a drop-cast $Fe_{3-x}Co_xO_4$ NC film exhibited both Coulomb blockade behavior and MR due to spin-dependent electron tunneling above the Coulomb blockade threshold voltage (V_T). The observed MR reached ~−80% in both H = 0.25 and 0.5 T, which suggests fulfillment of the m = 1 condition in the drop-cast $Fe_{3-x}Co_xO_4$ NC film. At 300 K, the thermal energy is larger than E_C, and hopping of spin-polarized electrons occurs between adjacent NCs. The drop-cast $Fe_{3-x}Co_xO_4$ NC film exhibited MR ~ −80% at 300 K in H = 0.2 T. So, the m = 1 condition persists even at 300 K. Herein we report MR ~ −80% at both 10 and 300 K for an oleic acid-coated $Fe_{2.7}Co_{0.3}O_4$ NC drop-cast film.

EXPERIMENTAL SECTION

Synthesis of $Fe_{2.7}Co_{0.3}O_4$ NCs and Fabrication of the NC Self-Assembled Film by Drop Casting. $Fe_{3-x}Co_xO_4$ NCs were synthesized from $Fe(acac)_3$ and $Co(acac)_2$ in a solution of dibenzylether and oleic acid according to an established procedure.[23] $Fe(acac)_3$, $Co(acac)_2$, dibenzylether, and oleic acid were combined in a 5:1:157:12 molar ratio and stirred vigorously for an hour at RT. The mixture was then refluxed at 573 K for half an hour. After cooling to RT, the NCs were precipitated from the crude solution by adding a 1:1 mixture of toluene/hexane followed by centrifugation. The precipitated NCs were washed with anhydrous chloroform and then dispersed in a weakly alkaline (pH = 10.4) aqueous solution. After stirring for 10 min, additional oleic acid (molar ratio of [Fe + Co]/$[C_{18}H_{34}O_2]$ = 1:42) was added to the solution with vigorous stirring. After stirring for another 20 min, 1 N HCl was added to neutralize the solution. After removal of the transparent solvent, the oleic acid-coated NCs were dispersed in hexane. The NCs were used without postpreparative size selection for fabrication of the NC self-assembled film by drop casting. The hexane colloidal suspensions were dropped onto a three-terminal electrode/MgO substrate and then dried at 573 K for half an hour at 100 Pa of air to yield an oleic acid-coated $Fe_{3-x}Co_xO_4$ NC self-assembled film.

The as-synthesized $Fe_{3-x}Co_xO_4$ NCs demonstrated an Fe/Co atomic ratio of 40:5 in energy dispersive X-ray (EDX) analysis, so the composition is denoted $Fe_{2.7}Co_{0.3}O_4$. (A sample EDX spectrum is provided in the Supporting Information.) A sketch of the three-terminal electrode/MgO substrate is shown in Figure 1a. First, the

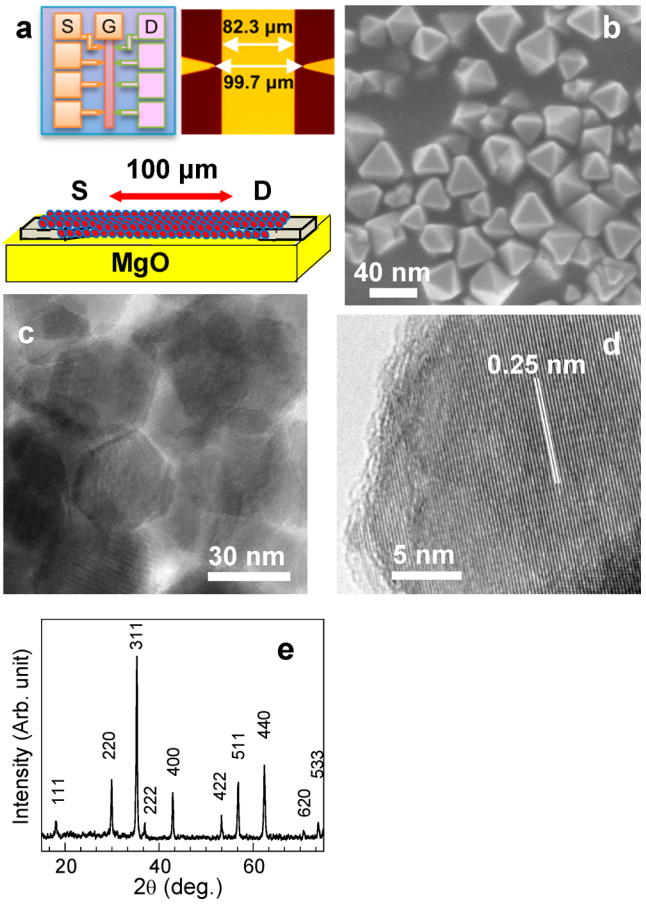

Figure 1. Sketch of the three-terminal electrode/MgO substrate (a, upper left), optical microscope image in the vicinity of the S-D electrodes (a, upper right), and sketch of the concept of the drop-cast NC film on the substrate as a two-terminal spin-polarized current switching device (a, lower). Representative SEM (b) and TEM (c) images of the as-synthesized $Fe_{2.7}Co_{0.3}O_4$ NCs. Representative high resolution TEM image of an as-synthesized $Fe_{2.7}Co_{0.3}O_4$ NC (d). XRD pattern of the as-synthesized $Fe_{2.7}Co_{0.3}O_4$ NCs (e).

substrate was patterned using photolithography to define an 80 μm long Au gate electrode. Subsequently, a 1 μm thick SiO_2 layer was deposited as a gate insulator via plasma chemical vapor deposition. Then, a further photolithography step was undertaken in order to define the Au source (S) and Ni drain (D) electrodes with an interelectrode distance of 100 μm.

Structural, Magnetic, and Magnetoelectric Characterization. The size and shape of the as-synthesized $Fe_{2.7}Co_{0.3}O_4$ NCs were examined using a HITACHI S-4800 scanning electron microscope (SEM) operated at an electron acceleration voltage of 1 kV, and a JEOL JEM-3100FEF transmission electron microscope (TEM) operated at an electron acceleration voltage of 300 kV. The crystal structure of the as-synthesized NCs was confirmed via X-ray diffraction (XRD) using a Rigaku CN2013 diffractometer with Cu Kα radiation.

Magnetic characterization was carried out using a superconducting quantum interference device (SQUID) magnetometer (Quantum Design, MPMS-5S). In order to acquire the temperature dependence of the dc magnetization ($M-T$) measurements, the sample was cooled from RT to 5 K in H = 0, and then H = 0.01 T was applied. The zero-field-cooled (ZFC) magnetization was recorded with increasing

temperature to 300 K. After the ZFC measurements, the sample was again cooled to 5 K in H = 0.01 T, and the field-cooled (FC) magnetization was then recorded, with temperature again increasing to 300 K. For magnetoelectric measurements, the S and D electrodes were bonded via gold wires to the Keithley Instruments Inc. Model 6487 Picoammeter/Voltage source. The $I-V$ character in H = 0 was measured first, and then that in $H \neq 0$. At 10 K, the $I-V$ characteristics in $H \neq 0$ were measured in fields of around H = 0.25 and 0.5 T.

RESULTS AND DISCUSSION

Figure 1a also shows our concept of a two-terminal spin-polarized current switching device. Although a three-terminal substrate was used to fabricate the self-assembled NC films, only two-terminal device characteristics are reported here. Spin- and dip-coating are the conventional methods for the preparation of NC films; however, these methods are usually not suitable for the assembly of a 2D superstructure of NCs in a film. Thus, a drop casting method was utilized in order to fabricate films of 2D ordered NC arrays by self-assembly. Such films of octahedral $Fe_{3-x}M_xO_4$ (M = Mn and Fe) NCs have been achieved via drop casting before.[3,4,24] Figure 1(b and c) shows typical SEM and TEM images of the as-synthesized $Fe_{2.7}Co_{0.3}O_4$ NCs, indicating both octahedra and elongated hexagons, respectively, approximately 30−40 nm in size. The triangular facets shown in the SEM image indicate that the {111} planes of octahedral NCs are well-developed. The anisotropic shape of the octahedron promotes self-assembly of the NCs in a highly packed and oriented structure, and the construction of a hexagonal NC lattice with collinear ferromagnetic moments.[3] Accordingly, $Fe_{2.7}Co_{0.3}O_4$ NC self-assembled films fabricated by drop casting would be expected to exhibit an SG transition near RT and a largely decreased G_0 for spin-polarized current flow.

The high resolution TEM image presented in Figure 1d demonstrates a lattice fringe of 0.25 nm, corresponding to the spacing of the (311) planes of the $Fe_{2.5}Co_{0.5}O_4$ crystal (ICDD 04-006-3507). As shown in Figure 1e, the XRD for the as-synthesized $Fe_{2.7}Co_{0.3}O_4$ NCs has a diffractogram attributable to an inverse spinel-type cubic lattice (space group $Fd\bar{3}m$) with a lattice parameter typical of oxide spinels (a = 0.84 nm). The crystallite size as estimated by Scherer's equation is 36 nm (radius r = 18 nm). Assuming an inter-NC space s of 4 nm due to oleic acid, the interelectrode distance of 100 μm corresponds to ca. 2500 NCs.

As a basis for considering the magnetic and electric characteristics of $Fe_{2.7}Co_{0.3}O_4$, the electronic structure of Fe_3O_4 with an inverse spinel-type crystal lattice is illustrated in the upper part of Figure 2. In the unit cell of the Fe_3O_4 crystal, Fe^{III} (S = 5/2) is distributed equally at both the A- and B-sites. The A- and B-sites are surrounded by oxygen tetrahedra and octahedra, respectively. If Fe^{II} (S = 2) and Fe^{III} alternately occupy the B-sites, then the Fermi level (E_F) locates in the spin-down t_{2g} band. As shown in the lower part of Figure 2, Co^{II} (S = 3/2) substituting for a third of the Fe^{II} sites, supplies two spin-down t_{2g} electrons. Thus, carriers hopping between the B-sites are still fully spin-polarized even in $Fe_{2.7}Co_{0.3}O_4$. Therefore, the spontaneous magnetization (M_s) per formula unit decreases from 4 μ_B to 3.7 μ_B, and the number of spin-polarized t_{2g} electrons per formula unit increases from 1 to 1.3 upon altering Fe_3O_4 to $Fe_{2.7}Co_{0.3}O_4$.

As shown in Figure 3a, the as-synthesized $Fe_{2.7}Co_{0.3}O_4$ NCs demonstrate a ferromagnetic hysteresis loop with H_c = 740 Oe, which agrees well with that reported by Yu et al.[16] In contrast,

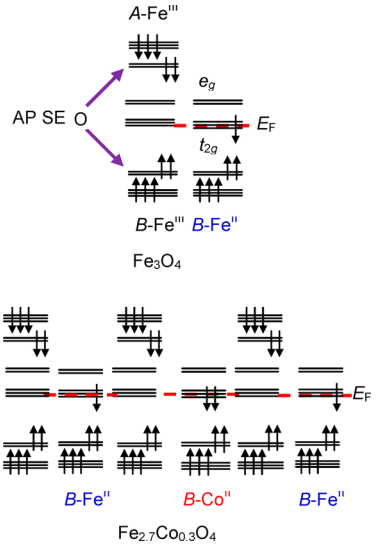

Figure 2. Upper illustration: The magnetic moments of Fe^{III} at the A- and B-sites are antiparallel (AP), and compensate for each other due to an antiferromagnetic superexchange (SE) interaction mediated by the apical oxygen (O) ion. The Fe^{III} and Fe^{II} 3d states with t_{2g} and e_g symmetry are separated by crystal-field splitting due to the octahedral coordination field of the B-site. The t_{2g} spin-down electron hops between the Fe^{III} and Fe^{II} at the B-site. Lower illustration: In the $Fe_{2.7}Co_{0.3}O_4$ crystal, Co^{II} is substituted for a third of the B-site Fe^{II} ions. Two spin-down t_{2g} electrons are supplied from the B-site Co^{II}. The sketch is for the ideal case of $Fe_{2.7}Co_{0.3}O_4$. Generally, Co can occupy also the A-site to some extent.

however, as-synthesized Fe_3O_4 NCs produced under the same conditions (except for a lack of $Co(acac)_2$) exhibit a sigmoidal curve with H_c = 70 Oe. The larger H_c for the as-synthesized NCs of $Fe_{2.7}Co_{0.3}O_4$ is what is expected for the chemical substitution, and suggests that the spin−orbit coupling of Co^{II} is more effective than that of Fe^{II}.[25]

As shown in Figure 3b, both the as-synthesized $Fe_{2.7}Co_{0.3}O_4$ NCs and the drop-cast $Fe_{2.7}Co_{0.3}O_4$ NC film are in the stable state, which means the relaxation time τ is larger than 100 s at 300 K. Such single-domain NCs have the size larger than the critical size at which H_C becomes zero. The blocking temperature T_B (= $KV/25k_B$), where V is the volume of each NC and k_B is the Boltzmann constant, of the as-synthesized $Fe_{2.7}Co_{0.3}O_4$ NCs is higher than 300 K. For each single-domain $Fe_{2.7}Co_{0.3}O_4$ NC, the thermal energy at 300 K is not sufficient to be superparameganetic. Higher T_B for the NC with constant V is resulted from larger K. The drop-cast $Fe_{2.7}Co_{0.3}O_4$ NC film exhibits a further enlargement in H_c to =1620 Oe. Hence, T_B of the drop-cast $Fe_{2.7}Co_{0.3}O_4$ NC film should be higher further than 300 K.

Based on the Stoner and Wolfarth model,[26] $K = H_C M_{1T}/2$ (here, M at 1 T is treated as M_s) of the as-synthesized NCs and the drop-cast NC film of $Fe_{2.7}Co_{0.3}O_4$ were estimated to be 1.4 × 10^4 J/m^3 and 3.0 × 10^4 J/m^3, respectively. The volume V = 2.0 × 10^{-23} m^3 was derived from the crystallite size. Thus, the anisotropy energy barrier KV, limiting free rotation of the magnetic moments away from the easy axis, amounts to 1.75 and 3.75 eV for the as-synthesized NCs and the drop-cast NC film of $Fe_{2.7}Co_{0.3}O_4$, respectively. The KV value of the drop-cast $Fe_{2.7}Co_{0.3}O_4$ NC film is much larger than the thermal energy at 300 K (26 meV). Therefore, the magnetic moments of the individual $Fe_{2.7}Co_{0.3}O_4$ NCs in the film cannot reverse direction rapidly as a result of the thermal energy. The enlarged

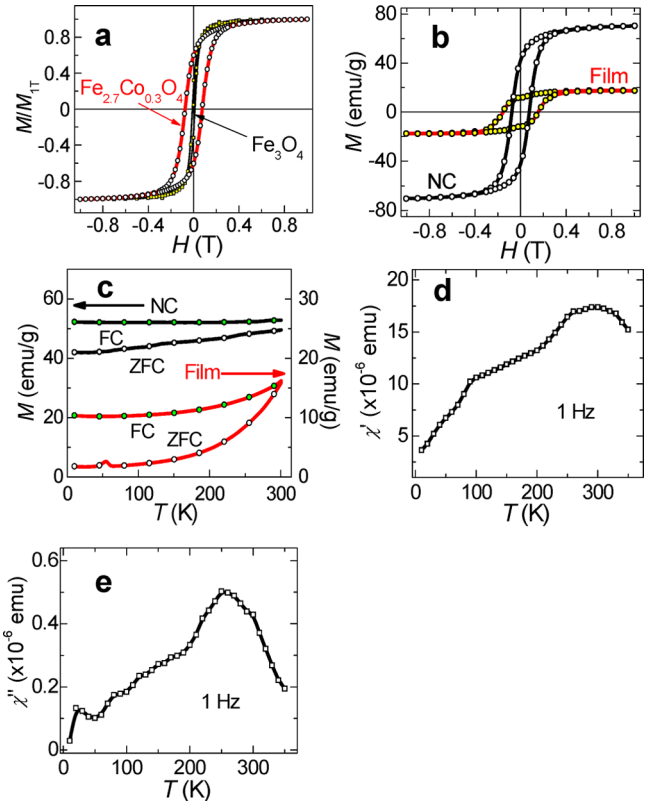

Figure 3. $M-H$ curves normalized to H = 1 T of the as-synthesized $Fe_{2.7}Co_{0.3}O_4$ and Fe_3O_4 NCs at 300 K (a). $M-H$ curves of the as-synthesized NCs and drop-cast NC film of $Fe_{2.7}Co_{0.3}O_4$ at 300 K (b). FC and ZFC dc M-T curves of the as-synthesized NCs and drop-cast NC film of $Fe_{2.7}Co_{0.3}O_4$ at H = 100 Oe (c). ZFC ac $\chi'-T$ (d) and $\chi''-T$ (e) curves at 1 Hz of the drop-cast $Fe_{2.7}Co_{0.3}O_4$ NC film.

magnetization reversal energy for the drop-cast $Fe_{2.7}Co_{0.3}O_4$ NC film is expected to bring about an enhancement in the spin-polarized current flow via the multiple magnetic junctions in $H \neq 0$.

For the drop-cast $Fe_{2.7}Co_{0.3}O_4$ NC film, M at H = 0.2 T reached ≈90% of that at H = 1 T, and M was almost saturated above H = 0.5 T. At H = 1 T, M (17 emu/g) of the drop-cast film amounted to 25% of that of the as-synthesized NCs (70 emu/g), and consequently, the mass percentage of $Fe_{2.7}Co_{0.3}O_4$ NC in the film is approximately 25%.

Figure 3c shows $M-T$ curves of the as-synthesized NCs and drop-cast NC film of $Fe_{2.7}Co_{0.3}O_4$, which demonstrate bifurcation of the FC and ZFC magnetizations at $T \geq 300$ K. For the as-synthesized $Fe_{2.7}Co_{0.3}O_4$ NCs, the FC magnetization remains almost constant below 300 K, whereas the ZFC magnetization is smaller, even at 300 K, and decreases almost linearly with decreasing temperature. For the drop-cast $Fe_{2.7}Co_{0.3}O_4$ NC film, the FC magnetization decreases gradually from 300 to 200 K and remains almost constant below 200 K. The ZFC magnetization bifurcates from the FC at 300 K, decreasing with decreasing temperature to 150 K, and then remains almost constant below 150 K. Such a cooling history-dependence of the dc magnetization is indicative of the slow dynamics common in self-assembled ferromagnetic NCs.[27,28] Figure 3d shows the temperature dependence of the real part of the ac susceptibility ($\chi'-T$) of the drop-cast $Fe_{2.7}Co_{0.3}O_4$ NC film. χ' peaks broadly at around 300 K, decreases gradually with decreasing temperature from 200 to 100 K, and then falls sharply below 100 K. Figure 3e shows the temperature dependence of the imaginary part of the ac susceptibility ($\chi''-T$) of the film. χ'' shows a broad peak at 250 K and a narrow peak at around 20 K. The χ'' anomaly at 20 K is an indication of the superspin glass transition in each isolated NC,[29] while that at 250 K, which is peculiar to the film, corresponds to the freezing of frustrated magnetic moments.

Electron transport via the oleic acid-coated $Fe_{2.7}Co_{0.3}O_4$ NCs requires $E_C = \{e^2/8\pi\varepsilon_0\varepsilon_r\}\{[1/r] - [1/(r+s)]\}$, where e and ε_0 are the elementary charge and the vacuum permittivity, respectively.[30] If the relative permittivity of oleic acid ε_r = 2 is assumed, E_C amounts to 3.6 meV. The thermal energy of electrons is not large enough to overcome E_C, which makes the drop-cast $Fe_{2.7}Co_{0.3}O_4$ NC film an insulator; however, a large bias $V > E_C$ opens conduction paths via the NCs in the film. At 10 K, the thermal energy of electrons is 0.9 meV, so the drop-cast $Fe_{2.7}Co_{0.3}O_4$ NC film demonstrates both Coulomb blockade and MR due to spin-dependent electron tunneling.

As shown in Figure 4a, the $I-V$ characteristics are asymmetric at 10 K. The asymmetry may be due to the

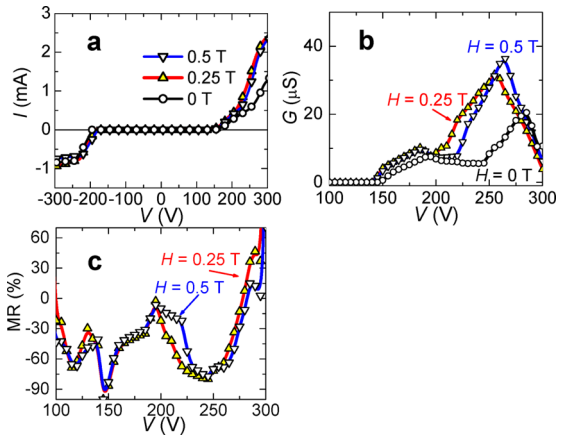

Figure 4. $I-V$ characteristics in H = 0, 0.25, and 0.5 T (a), G vs V plot (b), and MR vs V plot (c) of the drop-cast $Fe_{2.7}Co_{0.3}O_4$ NC film at 10 K.

nonmagnetic Au and ferromagnetic Ni electrode structure of the device. Additionally, spin-dependent electron tunneling is totally blocked in the range from −175 V (−70 mV/NC) to 150 V (60 mV/NC) due to local charging of the NCs by a single electron, despite the change in H. Outside of that range, electron tunneling paths between the S and D electrodes are opened, and the tunnel current starts to flow via the NCs in the film. As also seen in Figure 4a, below and above $V \approx 200$ V (80 mV/NC), I increases rather slowly and then rapidly, respectively, with increasing V. Just above V_T (150 V), a V larger than E_C was applied for the first time to the film, at which point electron tunneling occurs most likely along a single path or a small number of branches. When the V value is further increased, I flows between the S and D electrodes through multiple pathways, which branch out and reconnect.[31]

For the drop-cast $Fe_{2.7}Co_{0.3}O_4$ NC film, spin-dependent electron tunneling responds not only to V but also to H. If the magnetic moments of the NCs align in parallel due to an applied $H \neq 0$, G_H becomes larger than G_0 at $V > V_T$. Figure 4a demonstrates that for H = 0.25 and 0.5 T, I is enlarged at $V >$ 200 V to almost the same degree. Each G peak in Figure 4b corresponds to the tunneling of an electron through the excited

energy states of an $Fe_{2.7}Co_{0.3}O_4$ NC in H = 0, 0.25, and 0.5 T. The height and width of the G_H peak for 0.25 and 0.5 T were enlarged in the same way, and the position of the G_H peak for 0.25 and 0.5 T were lowered similarly by 20 V from ≈280 V (H = 0) to ≈260 V ($H \neq 0$). The number of electrons confined to a NC by E_C varies with H; in H = 0, it is small, and in $H \neq 0$, it is large. At V = 245 V, G_0 dips. Thus, MR at 10 K in both H = 0.25 and 0.5 T reaches −80% at V = 245 V, as shown in Figure 5c. The magnetic coupling between the NCs in the drop-cast

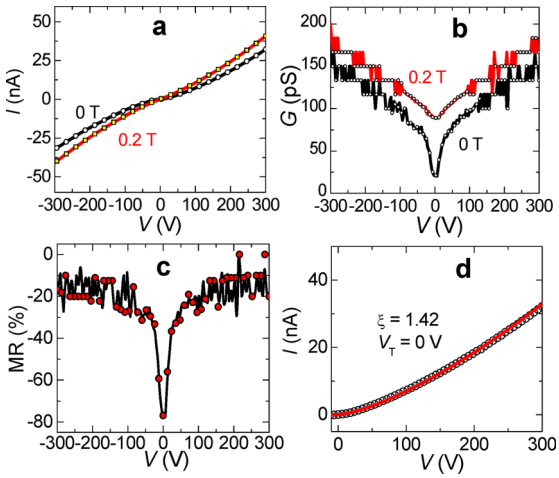

Figure 5. I−V characteristics in H = 0 and 0.2 T (a), G vs V plot (b), MR vs V plot (c), and fitting of the I−V curve in H = 0 T to estimate the ξ value (d) for the drop-cast $Fe_{2.7}Co_{0.3}O_4$ NC film at 300 K.

$Fe_{2.7}Co_{0.3}O_4$ NC film is enhanced by H = 0.25 and 0.5 T to almost the same degree. The spin-dependent electron tunneling probability increases rapidly above V = 200 V in the same way. Spin-polarized current flowing through multiple magnetic junctions is affected by competing dipolar interactions. The frustrated magnetic moments in percolating current paths give rise to a small G_0. An application of $H \neq 0$, which rotates the frustrated magnetic moments into mutual alignment (m = 1), results in a large G_H. The MR ∼ −80% in both H = 0.25 and 0.5 T indicates fulfillment of the m = 1 condition for the drop-cast $Fe_{3-x}Co_xO_4$ NC film.

At elevated temperature, G of the drop-cast $Fe_{2.7}Co_{0.3}O_4$ NC film is no longer determined by the Coulomb blockade. Because the thermal energy of electrons at 300 K is larger than E_C, the assumption that V_T = 0 V becomes rational. Since the frozen magnetic moments at low temperatures in percolating current paths thaw progressively with increasing temperature, the frustrated magnetic moments are probably still partially frozen, and yet cooperatively, randomly switching at 300 K. Thus, G_0 remains small even at 300 K, and H fulfilling the m = 1 condition enlarges G_H in the spin-polarized electron hopping between adjacent $Fe_{2.7}Co_{0.3}O_4$ NCs. Therefore, a large, negative MR at 300 K is also expected for the drop-cast $Fe_{2.7}Co_{0.3}O_4$ NC film.

As shown in Figure 5a, the drop-cast $Fe_{2.7}Co_{0.3}O_4$ NC film demonstrates nonlinear I−V characteristics at 300 K, which resemble intergranular tunneling conductance.[32] At every V, H = 0.2 T enlarges the I value and lowers the nonlinearity of the I−V curve. As seen in Figure 5b, G_0 and G_H were low and high, respectively. It is well-known that an anisotropic effect is absent in the MR of granular systems.[33] An H applied perpendicular to the film surface aligns the magnetic moments of the NCs parallel to each other and results in an enlargement of the spin-polarized current flowing through adjacent NCs. The G−V curves dip low around V = 0 and rise up sharply with increasing $|V|$. The G−V characteristic of a single interparticle tunneling junction is assumed to be proportional to the density of NC occupied states on the S side, and to that of empty states on the D side. Electron tunneling at different values of V is used to probe different energy ranges of the density of NC states above E_F on the D side. As is discussed above, 2500 NCs are estimated to lie between the S and D electrodes in this experiment, so the S−D bias voltage amounts to 0.12 V/NC at V = 300 V. Therefore, the 50 V half-width of the G−V peak mirrors the 20 meV-wide empty state in the conduction band of $Fe_{2.7}Co_{0.3}O_4$.

As shown in Figure 5c, the MR of the drop-cast $Fe_{2.7}Co_{0.3}O_4$ NC film reaches ∼−80% at 300 K in H = 0.2 T. An increase in the temperature should lessen the degree of spin-polarization near E_F, although a large negative MR (∼−80%) is still retained at 300 K. In 3D multiple junction systems, randomly distributed ferromagnetic NCs cannot yield an MR exceeding −50%, even if the m = 1 and P = 100% conditions are fulfilled.[1] Therefore, the dimensionality of the spin-polarized current flow paths was examined via power-law scaling[34] with $I \sim (V - V_T)^{\xi}$. This power law is related to the progressive opening of conduction channels. As shown in Figure 5d, the experimental I−V curve fits well with the critical exponent ξ = 1.4 when V_T = 0 V is assumed. The ξ values for 1D and 2D NC arrays have been analytically determined to be 1 and 5/3, respectively.[31] So, an experimental ξ value located between those of 1D and 2D NC arrays suggests that spin-polarized current flows through nearly 2D percolated paths among the self-assembled $Fe_{2.7}Co_{0.3}O_4$ NCs in the drop-cast film.

The symmetric and nonlinear I−V curve with V_T = 0 V suggests that the variable range hopping (VRH) conduction predominates in the transport at 300 K. In contrast to the spin-dependent tunneling conduction between adjacent NCs at 10 K, the conductance to a more distant state is favored in VRH, because of the smaller activation energy. The activation energy is proportional to an inverse of hopping distance. So, the nonmagnetic Au and ferromagnetic Ni electrode structure of the device scarcely influences on MR ∼ −80% at 300 K of the drop-cast $Fe_{2.7}Co_{0.3}O_4$ NC film.

CONCLUSION

$Fe_{2.7}Co_{0.3}O_4$ NCs, in which Co^{II} is partially substituted for Fe^{II} in Fe_3O_4, were employed to fabricate an oleic acid-coated $Fe_{2.7}Co_{0.3}O_4$ NC film using the spontaneous self-assembly phenomenon of colloidal particles. The drop-cast $Fe_{2.7}Co_{0.3}O_4$ NC film demonstrates a large H_c (1620 Oe), which is necessary for fulfilling the m = 1 condition, even at 300 K. At 10 K, the film exhibits both a Coulomb blockade and MR. Spin-dependent electron tunneling in both H = 0.25 and 0.5 T results in an MR ∼ −80% above V_T. Thermal energy brings about V_T = 0 V at 300 K, followed by hopping of spin-polarized electrons between adjacent NCs. At 300 K, the film exhibits MR ∼ −80% at $V \approx 0$ V in H = 0.2 T. Thus, the m = 1 condition persists even at 300 K. Fulfillment of the m = 1 and P = 100% conditions for $Fe_{2.7}Co_{0.3}O_4$ NC arrays gives rise to a large MR for the drop-cast film, which can offer very high performance for a spin-dependent current switching device.

Only two-terminal device characteristics of the drop-cast $Fe_{2.7}Co_{0.3}O_4$ NC film are reported, though the three-terminal electrode substrate used in this study is useful for the

fabrication of a top gate-type spin-dependent field-effect single electron transistor. In such a transistor, tuning of the top-gate voltage allows precise control of the number of electrons on an NC. V_T is tunable by the NC size, and I at outside of the Coulomb blockade range can be enhanced by $H \neq 0$. Interplay of spin-dependent transport, single electron charging, and field effect realizes a high performance spin transistor, which exhibits intriguing properties.

■ ASSOCIATED CONTENT

Supporting Information

X-ray emission spectrum of as-synthesized $Fe_{2.7}Co_{0.3}O_4$ NCs. This material is available free of charge via the Internet at http://pubs.acs.org/.

■ AUTHOR INFORMATION

Corresponding Author

*Email: kohiki@che.kyutech.ac.jp.

Notes

The authors declare no competing financial interest.

■ ACKNOWLEDGMENTS

S.K. thanks Mr. Y. Narada for assistance, Dr. H. Shimooka for the SEM, and the support of a Yoshida Research Grant for this work. This work was partly supported by the "Nanotechnology Platform Project" of the Ministry of Education, Culture, Sports, Science, and Technology, Japan.

■ REFERENCES

(1) Inoue, J.; Maekawa, S. Theory of Tunneling Magnetoresistance in Granular Magnetic Films. *Phys. Rev. B* **1996**, *53*, R11927−R11929.

(2) Yakushiji, K.; Mitani, S.; Takanashi, K.; Takahashi, S.; Maekawa, S.; Imamura, H.; Fujimori, H. Enhanced Tunnel Magnetoresistance in Granular Nanobridges. *Appl. Phys. Lett.* **2001**, *78*, 515−517.

(3) Kohiki, S.; Okada, K.; Mitome, M.; Kohno, A.; Kinoshita, T.; Iyama, K.; Tsunawaki, F.; Deguchi, H. Magnetic and Magnetoelectric Properties of Self-Assembled $Fe_{2.5}Mn_{0.5}O_4$ Nanocrystals. *ACS Appl. Mater. Interfaces* **2011**, *3*, 3589−3593.

(4) Kohiki, S.; Kinoshita, T.; Nara, K.; Akiyama-Hasegawa, K.; Mitome, M. Large Negative Magnetoresistance in an Oleic Acid-Coated Fe_3O_4 Nanocrystal Self-Assembled Film. *ACS Appl. Mater. Interfaces* **2013**, *5*, 11584−11589.

(5) Yanase, A.; Siratori, K. Band Structure in the High Temperature Phase of Fe_3O_4. *J. Phys. Soc. Jpn.* **1984**, *53*, 312−317.

(6) Zhang, Z.; Satpatahy, S. Electron States, Magnetism, and the Verwey Transition in Magnetite. *Phys. Rev. B* **1991**, *44*, 13319−13331.

(7) Poddar, P.; Fried, T.; Markovich, G. First-Order Metal-Insulator Transition and Spin-Polarized Tunneling in Fe_3O_4 Nanocrystals. *Phys. Rev. B* **2002**, *65*, 172405.

(8) Zeng, H.; Black, C. T.; Sandstrom, R. L.; Rice, P. M.; Murray, C. B.; Sun, S. Magnetotransport of Magnetite Nanoparticle Arrays. *Phys. Rev. B* **2006**, *73*, 020402 (R).

(9) Wang, W.; Yu, M.; Batzill, M.; He, J.; Diebold, U.; Tang, J. Enhanced Tunneling Magnetoresistance and High-Spin Polarization at Room Temperature in a Polystyrene-Coated Fe_3O_4 Granular System. *Phys. Rev. B* **2006**, *73*, 134412.

(10) Kant, K. M.; Sethupathi, K.; Rao, M. S. R. Role of Oxide Barrier in Intergranular Tunnel Junctions: An Enhanced Magnetoresistance in SiO_2 and ZnO-Coated Fe_3O_4 Nanoparticles Compacts. *J. Appl. Phys.* **2008**, *103*, 07F318.

(11) Wang, W.; He, J.; Tang, J. Enhanced Tunneling Magnetoresistance of Fe_3O_4 in a Fe_3O_4-Hexabromobenzene (C_6Br_6) Composite System. *J. Appl. Phys.* **2009**, *105*, 07B105.

(12) Wang, S.; Yue, F. J.; Wu, D.; Zhang, F. M.; Zhong, W.; Du, Y. W. Enhanced Magnetoresistance in Self-Assembled Monolayer of Oleic Acid Molecules on Fe_3O_4 Nanoparticles. *Appl. Phys. Lett.* **2009**, *94*, 012507.

(13) Taub, N.; Tsukernik, A.; Markovich, G. Inter-Particle Spin-Polarized Tunneling in Arrays of Magnetite Nanocrystals. *J. Mag. Mag. Mater.* **2009**, *321*, 1933−1938.

(14) Ziese, M.; Blythe, H. J. Magnetoresistance of Magnetite. *J. Phys.: Condens. Matter* **2000**, *12*, 13−28.

(15) Nlebedim, I. C.; Snyder, J. E.; Moses, A. J.; Jiles, D. C. Anisotropy and Magnetostriction in Non-Stoichiometric Cobalt Ferrite. *IEEE Trans. Magn.* **2012**, *48*, 3084−3087.

(16) Yu, Y.; Mendoza-Garcia, A.; Ning, B.; Sun, S. Cobalt-Substituted Magnetite Nanoparticles and Their Assembly into Ferrimagnetic Nanoparticle Arrays. *Adv. Mater.* **2013**, *25*, 3090−3094.

(17) Solano, E.; Perez-Mirabet, L.; Martinez-Julian, F.; Guzmán, R.; Arbiol, J.; Puig, T.; Obradors, X.; Yañez, R.; Pomar, A.; Ricart, S.; Ros, J. Facile and Efficient One-Pot Solvothermal and Microwave-Assisted Synthesis of Stable Colloidal Solutions of MFe_2O_4 Spinel Magnetic Nanoparticles. *J. Nanopart. Res.* **2012**, *14*, 1034−1049.

(18) Sun, S.; Zeng, H.; Robinson, D. B.; Raoux, S.; Rice, P. M.; Wang, S. X.; Li, G. Monodisperse MFe_2O_4 (M = Fe, Co, Mn) Nanoparticles. *J. Am. Chem. Soc.* **2004**, *126*, 273−279.

(19) Tadmor, R.; Rosensweig, R. E.; Frey, J.; Klein, J. Resolving the Puzzle of Ferrofluid Dispersants. *Langmuir* **2000**, *16*, 9117−9120.

(20) Murray, C. B.; Kagan, C. R.; Bawendi, M. G. Synthesis and Characterization of Monodisperse Nanocrystals and Close-Packed Nanocrystal Assemblies. *Annu. Rev. Mater. Sci.* **2000**, *30*, 545−610.

(21) Prasad, B. L. V.; Sorensen, C. M.; Klabunde, K. J. Gold Nanoparticle Superlattices. *Chem. Soc. Rev.* **2008**, *37*, 1871−1883.

(22) Rybchenko, S. I.; Fujishiro, Y.; Takagi, Y.; Awano, M. Effect of Grain Boundaries on the Magnetoresistance of Magnetite. *Phys. Rev. B* **2005**, *72*, 054424.

(23) Kim, D.; Lee, N.; Park, M.; Kim, B. H.; An, K.; Hyeon, T. Synthesis of Uniform Ferrimagnetic Magnetite Nanocubes. *J. Am. Chem. Soc.* **2009**, *131*, 454−455.

(24) Zhang, L.; Wu, J.; Liao, H.; Hou, Y.; Gao, S. Octahedral Fe_3O_4 Nanoparticles and Their Assembled Structures. *Chem. Commun.* **2009**, 4378−4380.

(25) Jin, C.; Li, P.; Mi, W. B.; Bai, H. L. Magnetocrystalline Anisotropy-Dependent Six-Fold Symmetric Anisotropic Magnetoresistance in Epitaxial $Co_xFe_{3-x}O_4$ Films. *Europhys. Lett.* **2012**, *100*, 27006.

(26) Stoner, C.; Wohlfarth, E. P. A Mechanism of Magnetic Hysteresis in Heterogeneous Alloys. *Philos. Trans. R. Soc. London* **1948**, *Ser. A 240*, 599−642.

(27) Doman, J. L.; Fiorani, D.; Trone, E. Magnetic Relaxation in Small Particles Systems. *Adv. Chem. Phys.* **1997**, *98*, 283−494.

(28) Mydosh, J. A. *Spin Glasses: An Experimental Introduction*; Taylor & Frances: London, 1993.

(29) Suzuki, M.; Fullem, S. I.; Suzuki, I. S.; Wang, L.; Zhong, C.-J. Observation of Superspin-Glass Behavior in Fe_3O_4 Nanoparticles. *Phys. Rev. B* **2009**, *79*, 024418.

(30) Abeles, B.; Sheng, P.; Coutts, M. D.; Arie, Y. Structural and Electrical Properties of Granular Metal Films. *Adv. Phys.* **1975**, *24*, 407−461.

(31) Middleton, A. A.; Wingreen, N. S. Collective Transport in Arrays of Small Metallic Dots. *Phys. Rev. Lett.* **1993**, *71*, 3198−3201.

(32) Simmons, J. G. Generalized Formula for the Electric Tunnel Effect between Similar Electrodes Separated by a Thin Insulating Film. *J. Appl. Phys.* **1963**, *34*, 1793−1803.

(33) Tripathy, D.; Adeyeye, A. O.; Shannigrahi, S. Magnetic and Tunneling Magnetoresistive Properties of an All-Oxide Fe_3O_4−Al_2O_3 Granular System. *Phys. Rev. B* **2007**, *76*, 174429.

(34) Parthasarathy, R.; Lin, X. M.; Jaeger, H. M. Electronic Transport in Metal Nanocrystal Arrays; The Effect of Structural Disorder on Scaling Behavior. *Phys. Rev. Lett.* **2001**, *87*, 186807.